AIAA JOURNAL
Vol. 32, No. 3, March 1994

Technical Notes

TECHNICAL NOTES are short manuscripts describing new developments or important results of a preliminary nature. These Notes cannot exceed 6 manuscript pages and 3 figures; a page of text may be substituted for a figure and vice versa. After informal review by the editors, they may be published within a few months of the date of receipt. Style requirements are the same as for regular contributions (see inside back cover).

High Angle-of-Attack Airfoil Performance Improvement by Internal Acoustic Excitation

Fei-Bin Hsiao*
National Cheng Kung University, Tainan, Taiwan, Republic of China
and
Rong-Nan Shyu† and Ray C. Chang‡
Chung-San Institute of Science and Technology, Taichung, Taiwan, Republic of China

I. Introduction

THE acoustic excitation technique has been widely used in boundary layer and shear flow control for many decades. Invariably, aerodynamic performance about a wing is improved due to an acoustically excited flowfield induced entrainment of momentum exchange in the boundary layer close to the wing surface.[1-3] The majority of previous studies on airfoil performance improvement always focused on low post-stalled angles, where separated shear flow around the leading-edge airfoil reattaches to the surface after acoustic excitation.[4,5] An application of a similar methodology to airfoils possessing high angles of attack beyond the stall angle, unfortunately, fails to reveal the effects and the possible mechanism of airfoil performance enhancement. In a detailed study of internal acoustic excitation on aerodynamic performance improvement about a stalled airfoil, Hsiao et al.[3] and Chang et al.[4] found that, at low post-stalled angles of attack, lift was increased with drag being reduced as long as the excitation frequency is locked in to the instability frequency of the separated shear layers, and excitation was located near the separation point of the boundary layer. However, at high angles of attack (AOA), the effectiveness of the shear layer instability frequency is still uncertain and deserves further investigation. This Note, therefore, emphasizes the internal acoustic excitation on the stalling airfoil performance improvement with angles of attack beyond 24 deg.

II. Experimental Setup

The experiments were conducted in a suction, open-circuited wind tunnel containing a 3×4 ft test section. An airfoil model of 30.48 cm in chord C with a NACA 63_3-018 cross section was used for velocity and pressure measurements. The acoustic fluctuations generated by a loudspeaker were funneled into the interior of the model and then ejected into the flowfield through a slot 0.8 mm in width located at 1.25% chord from the airfoil's leading edge. Throughout the measurements, the freestream velocity U_∞ was kept at 15.5 m/s, which corresponds to a Reynolds number of 3.1×10^5. A detailed description of the experimental setup and procedures is contained in Refs. 3 and 4.

Received May 5, 1992; presented as Paper 92-02-012 at the DGLR/AIAA 14th Aeroacoustics Conference, Aachen, Germany, May 11–15, 1992; revision received Aug. 5, 1993; accepted for publication Aug. 6, 1993.

*Professor, Institute of Aeronautics and Astronautics. Member AIAA.
†Research Scientist, Aeronautical Research Laboratory.
‡Senior Research Scientist, Aeronautical Research Laboratory.

III. Results and Discussion

A. High Post-Stalled Angle Airfoil Performance After Excitation

Separated flow can be effectively controlled when the excitation frequency is tuned to, and the perturbation source is applied at, the shear layer instability frequency, as obtained by Hsiao et al.[3] However, if high post-stalled angles are employed, e.g., AOA > 24 deg, the effectiveness of forcing becomes degenerative due to an increased adverse pressure gradient. Under these conditions, even high-amplitude forcing barely reattaches the boundary layer to the airfoil surface. Since the flow pattern over the high post-stalled angle airfoil tends to form a series of shedding vortices in the

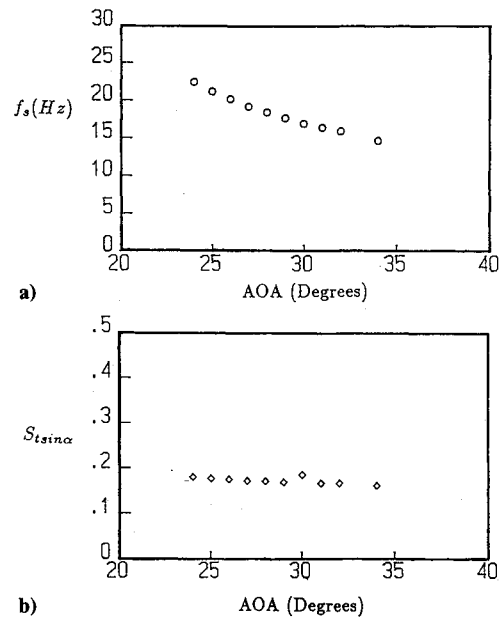

Fig. 1 a) Vortex-shedding frequencies and b) Strouhal number vs AOA for $Re_c = 3.1 \times 10^5$.

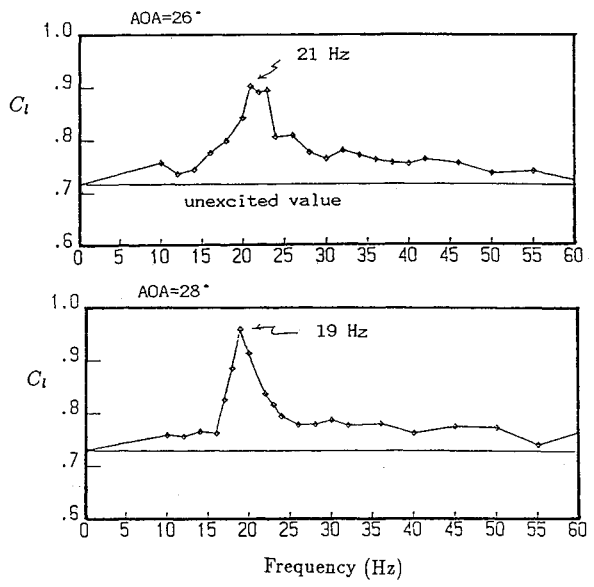

Fig. 2 Variation in the lift coefficient with excitation frequency at AOA of 26 and 28 deg.

wake, the vortex-shedding frequency is expected to be an effective forcing frequency in controlling aerodynamic performance. Note in the low post-stalled regions (AOA of 20–24 deg) the absence of well-defined peaks, which reflects the fact that no significant vortex structure has formed behind the airfoil. At higher angles of attack, on the other hand, a narrow-banded peak is obtained due to shedding vortex formation. This peak frequency is known as the shedding instability frequency f_s and decreases with an increase of the angle of attack. According to Roshko,[5] the Strouhal number of the vortex-shedding frequency $St_{\sin\alpha}$ is given by

$$St_{\sin\alpha} = \frac{f_s C \sin\alpha}{U_\infty} = 0.17 \sim 0.19$$

where α is the angle of attack. The measured results are in good agreement with this relationship as shown in Figs. 1a and 1b.

Variations in the lift coefficient with respect to the excitation frequency for AOA of 26 and 28 deg are shown in Figs. 2a and 2b. A comparison of these figures reveals that the most effective frequency for improving aerodynamic performance varies depending on the angle of attack and is correlated with the vortex-shedding instability frequency in the wake. Thus, for high post-stalled angle airfoil performance improvement, enhancement of vortex shedding instability is the dominant mechanism in flow control. Moreover, in comparison with lower AOA, the effective forcing frequency range is more restricted, corresponding to the narrow-banded vortex-shedding frequency peak.

B. Effectiveness of Vortex-Shedding Frequency Forcing at High AOA

Averaged pressure distributions with and without effective forcing at AOA of 26 and 28 deg are shown in Figs. 3a and 3b, respectively. Note that whereas the pressure distribution on the airfoil's lower surface does not change under excitation, over the upper surface, however, a reduction in base pressure occurs after forcing. Under excitation conditions, leading-edge separation still occurs on the airfoil, with the flow pattern remaining unattached to the airfoil surface. This result is in contrast to that for the low AOA airfoil control where the separated flow is partially reattached after forcing.[3]

Energy spectra of velocity fluctuations in the wake region at different forcing frequencies for 26-deg AOA are shown in Fig. 4. Note that the natural shedding frequency occurs at 20.5 Hz in the absence of excitation, whereas under a 30-Hz excitation, peak frequency shifts to 21.25 Hz due to nonlinear interaction, with peak energy being slightly reduced. Thus, it is reasonable to believe that forcing perturbations do not change the nature of the vortex-shedding process but rather synchronize the event at the applied forcing frequency; results are in good agreement with those of Blevins,[6] who examined the effect of sound on vortex shedding from a cylinder. A 20.5-Hz excitation at the vortex-shedding frequency not only reduces the vortex-shedding frequency's bandwidth but also concentrates vortex energy at the applied frequency. Thus, we can conclude that periodic perturbations possess the ability to synchronize the frequency of, and increase the strength of, vortices shed from the airfoil when the forcing frequency closely matches that of the natural shedding instability in the wake.

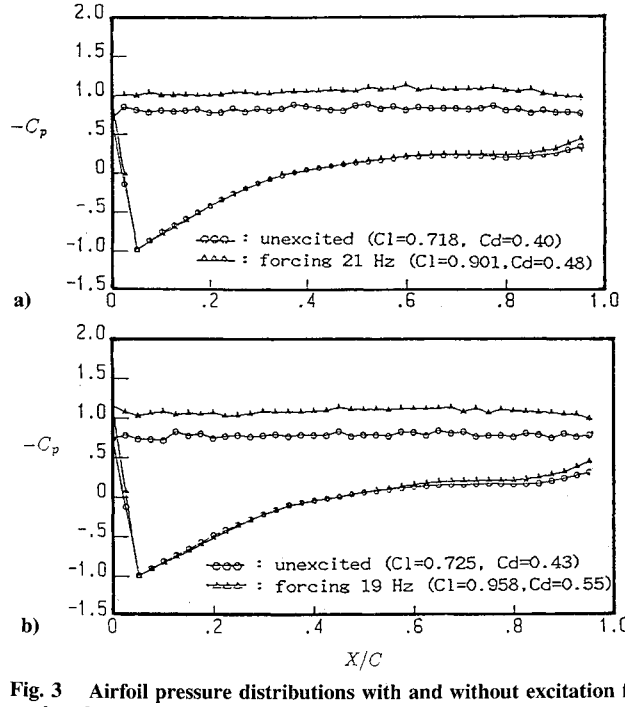

Fig. 3 Airfoil pressure distributions with and without excitation for angles of attack: a) 26 deg and b) 28 deg.

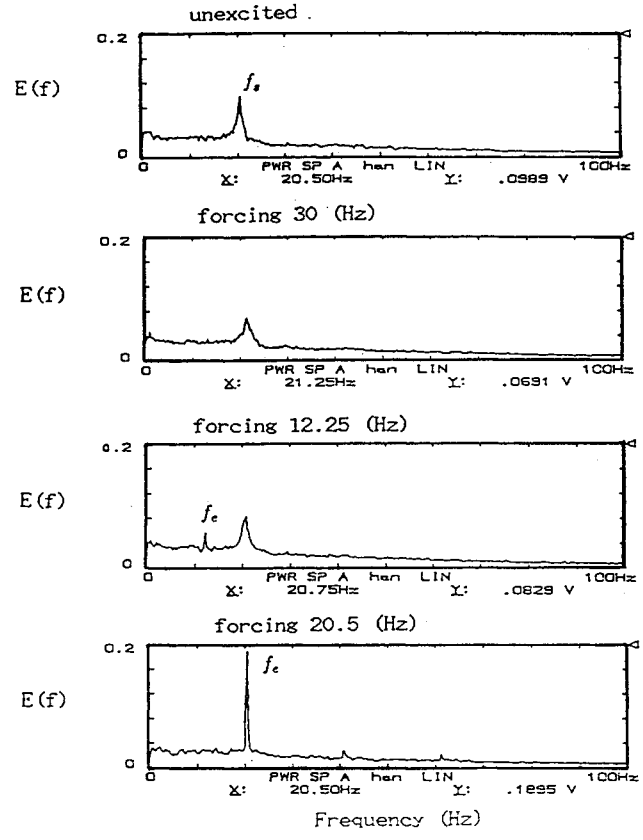

Fig. 4 Energy spectra of velocity fluctuations in the wake at different forcing frequencies and at 26-deg angle of attack.

IV. Concluding Remarks

This Note studies the technique of internal acoustic excitatin on improving the stalling airfoil performance at high angles of attack. As forcing at the shear layer instability frequency is effective for a reattached flow at a low AOA airfoil, the most effective forcing frequency in terms of improving airfoil performance matches the vortex-shedding frequency for the stalled airfoil having an angle of attack greater than 24 deg. Under the effective excitation condition, not only the flow keeps separated at the leading edge of the airfoil, but also the vortical structures are formed prematurely on the upper surface of the airfoil, achieving higher lift and drag due to decreased base pressure over the airfoil's upper surface.

Acknowledgment

The financial support of this work by the National Science Council of the Republic of China under Contract NSC79-0210-D006-03 is gratefully acknowledged.

References

[1]Collins, F. G., "Boundary Layer Control on Wings Using Sound and Leading-Edge Serrations," *AIAA Journal*, Vol. 19, No. 2, 1981, pp. 129, 130.

[2]Zaman, K. B. M. Q., Bar-Sever, A., and Mangalam, S. M., "Effect of

Acoustic Excitation on the Flow Over a Low-*Re* Airfoil," *Journal of Fluid Mechanics*, Vol. 182, Sept. 1987, pp. 127–148.

[3]Hsiao, F. B., Liu, C. F., and Shyu, J. Y., "Control of Wall-Separated Flow by Internal Acoustic Excitation," *AIAA Journal*, Vol. 28, No. 8, 1990, pp. 1440–1446.

[4]Chang, R. C., Hsiao, F. B., and Shyu, R. N., "Forcing Level Effect of Internal Acoustic Excitation on the Improvement of Airfoil Performance," *Journal of Aircraft*, Vol. 29, No. 5, 1992, pp. 823–829.

[5]Roshko, A., "On Drag and Shedding Frequency of Two-Dimensional Bluff Bodies," NACA-TN-3169, 1954.

[6]Blevins, R. D., "The Effect of Sound on Vortex Shedding From Cylinders," *Journal of Fluid Mechanics*, Vol. 161, Dec. 1985, pp. 217–237.

Using the Liou-Steffen Algorithm for the Euler and Navier-Stokes Equations

Lorenzo Bergamini* and Pasquale Cinnella†
Mississippi State University,
Mississippi State, Mississippi 39762

Introduction

RECENT years have witnessed the affirmation of both flux-vector and flux-difference techniques[1] for the accurate numerical simulation of compressible fluid flows. Two of the most popular schemes have been proposed by Roe and Van Leer, respectively, and are widely utilized for both inviscid and viscous calculations. However, robustness problems have been experienced by some users of the Roe scheme,[2] and the Van Leer technique has been shown to be too dissipative for viscous calculations.[3]

In a related study,[4] the authors investigated the advantages and drawbacks of a new flux-splitting scheme proposed by Liou and Steffen,[3] when compared with the algorithms developed by Van Leer and Roe. The comparison involved inviscid and viscous flows in one and two space dimensions. In the following, a brief summary of those findings is given.

Numerical Formulation

The governing equations for viscous flows are discretized in space using upwind technology, in conjunction with a finite volume approach.[5] Three different flux-splitting schemes are implemented for the discretization of the inviscid fluxes, and second-order central differences are utilized for the viscous fluxes.

Two different techniques have been implemented to advance the numerical solution in time: an explicit m-step Runge-Kutta algorithm[5] and a fully implicit modified two-step factorization technique.[6] The Runge-Kutta algorithm with two or more steps is second-order accurate in time and is particularly useful for unsteady simulations. The implicit formulation can be made second-order accurate in time by means of inner iterations to the unsteady residual.[6]

The convergence rate to steady-state solutions is enhanced by means of mesh sequencing, whereby the computation is started impulsively on a coarse grid, and after a convenient residual reduction, the partially converged solution is extrapolated to a finer grid. This technique allows for an inexpensive resolution of the initial transient, which is typically responsible for a large portion of the total CPU time required for a given simulation.

Three flux-splitting schemes are compared in the following. The first one was originally proposed[1] by Van Leer. The second one was proposed by Liou and Steffen,[3] is similar to Van Leer's, and is also based on the splitting of a velocity parameter and the pressure. The splitting formulas are the same ones employed by the previous scheme, although a lower-order splitting for the pressure is introduced and recommended by the authors over the "standard" formula. The algorithm differs from the previous one in the treatment of the convective contributions to the inviscid fluxes. Finally, an approximate Riemann solver of the Roe type[1] is implemented and compared with the previous techniques.

Presented as Paper 93-0876 at the AIAA 31st Aerospace Sciences Meeting, Reno, NV, Jan. 11–14, 1993; received March 13, 1993; revision received Aug. 10, 1993; accepted for publication Aug. 25, 1993.

*Research Assistant, Engineering Research Center for Computational Field Simulation, P.O. Box 6176.

†Assistant Professor, Department of Aerospace Engineering, P.O. Box 6176. Member AIAA.

Numerical Results

Numerical results for seven test cases, four inviscid and three viscous, were obtained in a related study.[4] The explicit two-step Runge-Kutta time integration scheme was adopted for the unsteady cases and the fully implicit modified two-step algorithm for the steady results. Unless otherwise stated, the space discretization was second-order accurate. The Van Leer limiter[6] was employed to correct the extrapolation of the primitive variables, which is necessary for the determination of left and right states to be utilized in the splitting algorithms, according to a Monotone Upstream-Centered Schemes for Conservation Laws (MUSCL) type logic.[7]

In the following, the major features of two of those test cases will be detailed.

Shock Reflection off of a Solid Wall

A shock tube simulation was selected as a simple unsteady test case with a known exact solution. The pressure and density ratios were selected to be 10:1, consequently, the temperature ratio between driver and driven sections was 1. The calculation utilized 400 points over a distance of 1 m, with the initial discontinuity located at a distance of $x=0.25$. The nondimensional time step utilized to advance the solution was $\Delta t=5\times10^{-4}$, and the reference values chosen for the nondimensionalization were the density and speed of sound in the driven section. The maximum Courant-Friedrichs-Lewy (CFL) number registered was of the order of 0.4.

The calculation was continued until the shock reached the end of the tube and reflected off of it. A solid wall boundary condition was imposed. Both characteristic-variable boundary conditions[8] and a straightforward imposition of zero pressure gradients/zero velocity at the wall were implemented, and the final results were insensitive to the choice made. The same boundary conditions were employed for all three techniques.

Figure 1 shows temperature plots for the three schemes at a nondimensional time $t=0.6$, which corresponds to conditions after reflection at the wall but before impact between the reflected shock and the contact discontinuity; Fig. 2 depicts temperature at time $t=0.725$, after the impact with the contact discontinuity but before contact with the expansion region. The light line represents the exact solution. The heavy line represents the prediction from

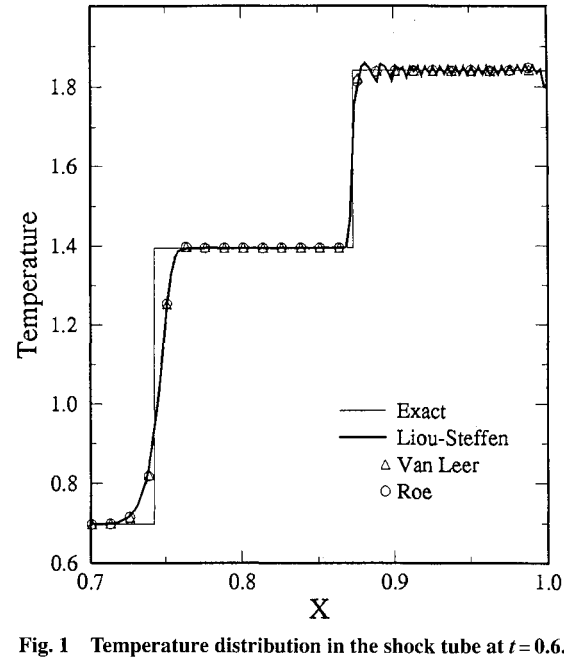

Fig. 1 Temperature distribution in the shock tube at $t=0.6$.